An Actuated Indenter for Characterization of Soft Tissue Towards Human-Centered Design*

Saad N. Yousaf[1], Keya Ghonasgi[1], Paria Esmatloo[1], and Ashish D. Deshpande[1]

***Abstract*—The viscoelastic properties of human soft tissue influence the nature of interaction at attachment points in wearable devices. Characterizing these properties is especially critical for understanding physical human-robot interaction (pHRI) for exoskeleton design, prosthetics, and similar fields. This paper presents the design and control of a novel actuated indenter for the measurement of human soft tissue properties. The accuracy of position (0.025 mm) and force (111 mN) measurements allows for repeatable and controlled tissue deformation and monitoring at 36 different angular locations (10° increments). Controlled indentation displacement with force feedback is used in three types of applications on a human subject's forearm. The soft tissue stiffness profile, viscoelastic relaxation behavior, and frequency domain response are measured. The ability to perform multiple characterizations with one indenter device broadens the scope of a human-centered approach to design, modeling, and perception as they relate to pHRI interfaces.**

I. Introduction

In wearable robotic devices, studying physical human-robot interaction (pHRI) is critical for understanding how forces are transmitted and perceived at attachment interfaces. Human soft tissue properties such as stiffness, viscoelasticity, and detection thresholds are important factors in pHRI behavior. Specifically, elastic stiffness determines how soft tissue will displace in response to various forces and can be used to inform the design of ergonomic wearable attachment interfaces [1]. Viscoelastic properties capture the dynamic behavior of human soft tissue and have been used in conjunction with MRI data and inverse FEA to build models of human skin and its underlying layers [2], [3], [4]. Detection thresholds of mechanical stimuli through soft tissue determine how distinct interactions are perceived by the human user [5], [6], [7]. While indentation is often used in these measurements, no single device has been proposed which is versatile enough to perform the different characterizations necessary for understanding the range of human soft tissue properties.

Many indenters have been designed as hand-held devices in which the operator applies force when indenting soft tissue [8], [9]. While these devices are easy to use, they lack the ability to control the direction, location, and rate of indentation that is necessary for accurate and repeatable measurements. For example, algometers, which are used to measure pressure pain threshold (PPT) via indentation, are generally hand-held devices. Alternatively, actuated indentation provides a higher fidelity of measurements and allows for more detailed characterizations of human soft tissue. Existing indenters in this category either include a structural base [10], [11], [12], [13] or are mounted to robotic arms [1], [14]. The standard indenter experiment characterizes the stiffness profile of soft tissue by measuring the force-displacement response, as done in [1], [11], [12], [13]. In an attempt to define more in-depth viscoelastic properties, indenters have also been used to measure soft tissue relaxation behavior [10], [14]. From a haptics perspective, indenters have been used to understand tactile perception when indenting with a small displacement [6] or at different frequencies [5], [7].

In this paper, we present an actuated indenter (Fig. 1) that

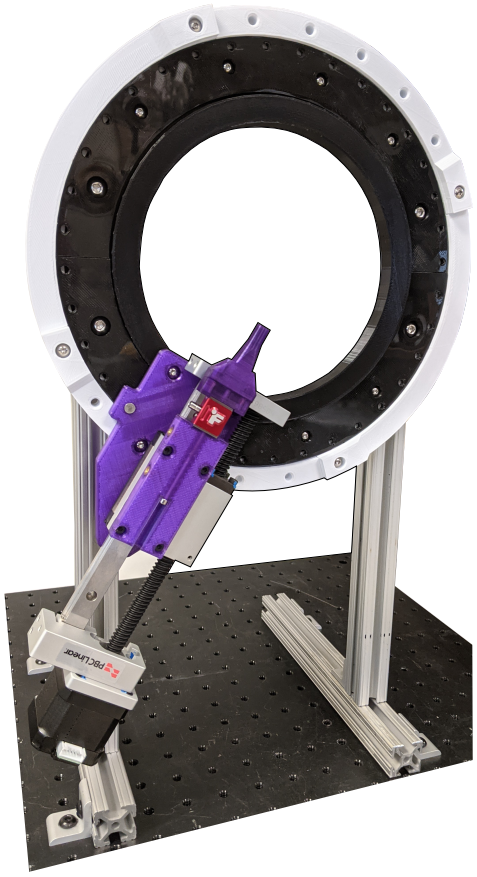

Fig. 1: Indenter assembly with the linear indentation carriage mounted on the rotating ring structure, which can be moved at the base. The human limb is placed through the rotating ring and grounded during characterization measurements.

*An earlier version of the indenter device presented in this paper was used in another AIM submission. In that work, the older indenter was used to collect data that was used in a simulation model.

This work was funded, in part, by the National Science Foundation (NSF) grant numbers 2019704 and 1941260, as well as the NSF Graduate Research Fellowship Program (GRFP) grant number DGE-1610403.

[1]S.N. Yousaf, K. Ghonasgi, P. Esmatloo, and A.D. Deshpande are with the Department of Mechanical Engineering, The University of Texas at Austin, Austin, TX 78712, USA. ashish@austin.utexas.edu

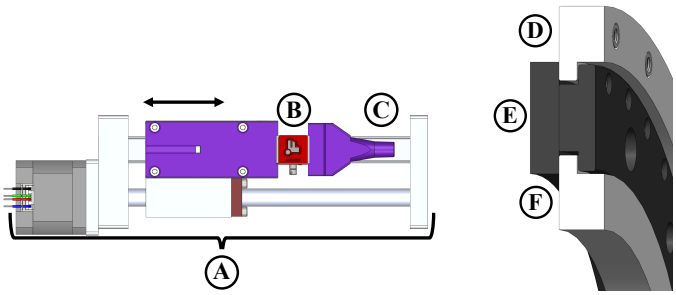

(a) Front View (b) Cross Section

Fig. 2: Linear indentation carriage module includes: (A) linear carriage driven by a stepper motor, (B) single-axis load cell for force measurement, and (C) indenter head that interfaces with soft tissue. Rotating ring structure module includes (D) outer ring, (E) grounded center ring, and (F) inner ring. The rotating components (white) slide in the grounded center ring (black).

can characterize a variety of soft tissue properties around a human limb. The control of indentation displacement with accurate force feedback broadens characterization beyond stiffness and allows the device to assess dynamic properties. The novel contribution of the device lies in its ability to perform multiple types of indentation experiments, including stiffness, viscoelastic relaxation, and high-frequency response, while also having a low-profile that enables measurement at many locations on different human limbs. This makes the device an important tool for developing a human-centered interface design process, as showcased in this paper.

II. Indenter Device Design

The indenter device consists of two main modules: a linear indentation carriage and a rotating ring structure.

A. Module 1: Linear Indentation Carriage

The first module (Fig. 2a) consists of an actuated linear carriage, a single-axis load cell, and the indenter head. The linear carriage (Compact Series, PBC Linear) is actuated with an integrated NEMA 17 stepper motor and moves 5 mm per revolution of the lead screw. It has a stroke of 100 mm, which is sufficiently larger than the indentation distance (typically less than 20mm [10], [15]). The system is controlled with a TB6600 stepper motor driver at the standard resolution of 200 steps per revolution (0.025 mm per step). However, the motor driver allows for micro-stepping up to 6400 steps per revolution (0.00078 mm per step) which can be used if higher displacement accuracy is required instead of indentation speed. The motor driver interfaces with a USB data acquisition device (NI 6356, National Instruments) through two digital output channels.

The single-axis load cell (LSB205, Futek) is rated for a maximum load of 44.5 N (10 lbs). The highest indentation forces expected at human limbs such as the forearm and the upper arm are 20-25 N based on PPT measures reported in literature [16]. The measurement errors for nonlinearity, hysteresis, and nonrepeatability are 0.1%, 0.1%, and 0.05% of the rated output, respectively, resulting in a maximum overall error of 0.111 N. The load cell is used with a compression calibration performed by the manufacturer. The force measurement is acquired through a USB load cell amplifier (USB220, Futek) with a sampling frequency that can be specified between 60 Hz and 6400 Hz. Both the load cell and the stepper motor interface with a computer through MATLAB (Mathworks), allowing the operator to implement different protocols for soft tissue characterization.

The components of the linear indentation carriage come together with 3D prints made from polyactic acid (PLA) filament, the most important of which is the indenter head. Previous research has shown that the shape and size of the indenter head affects measurement of soft tissue properties [17]. In this paper, the standard indenter head used is cylindrical in shape with an 8 mm diameter and rounded edges for user comfort. The modular assembly allows the indenter head to be easily switched, allowing for this additional factor to be studied during soft tissue characterization.

B. Module 2: Rotating Ring Structure

The second module of the device presented in this paper is the rotating ring structure which determines the location and orientation of indentation. A cross section view is shown in Fig. 2b, consisting of a center ring grounded to an aluminum frame along with an inner ring and outer ring that slide around the circumference. The inner and outer rings are coupled through a single piece that also interfaces with the base of the linear indentation carriage. The inner diameter of the overall rotating ring structure is 160 mm, accommodating most human limbs. Holes for a 4 mm dowel pin on the grounded center ring are spaced in 10° increments and allow the linear indentation carriage to be placed at one of 36 different angular orientations. The aluminum frame can also be moved along the length of the limb to capture soft tissue properties along a larger surface area by adjusting the grounding location at the base of the aluminum frame.

Two strapped cuffs are used alongside the rotating ring structure to ground the human limb. The size and shape of the cuffs will vary depending on the specific region of the body being tested. For the forearm, we use a larger cuff near the elbow and a smaller cuff at the wrist, both of which are intended to ground the arm by strapping near bony areas and not interfere by influencing soft tissue near the point of indentation. All parts for the rotating ring structure and the grounding cuffs are 3D printed from polyactic acid (PLA) filament and mounted on aluminum frames.

III. Experiments

A. Validation of Instrumentation

The accuracy of position and force measurements from the indenter device is validated with ground truth measurements from external sensors. The linear indentation carriage module is attached to a fixed base with the indenter head placed in series with two parallel springs. As the linear carriage

actuates forward, force from spring compression is imparted onto the indenter's single-axis load cell and validated with ground-truth measurements from a six-axis load cell (RFT40, Robotous) placed at the base of the springs. Simultaneously, a linear encoder (EM1, US Digital) records the position of the linear carriage, validating the displacement measurement derived from stepper motor counts. During each of the three trials, the linear carriage indents until the single-axis load cell reaches a threshold force of 10 N.

B. Example Applications

A pilot study is conducted with a single human subject. The results of this pilot study do not allow for drawing generalizable conclusions about human properties across subjects and are instead presented as a demonstration of the various characterizations of human soft tissue enabled by the use of the indenter device. The setup shown in Fig. 3a is used for all experiments in this section with the forearm anchored near the bony areas of the wrist and elbow. The subject is instructed to relax their muscles during all experiments unless told otherwise. All experiments use a standard 8mm diameter cylindrical indenter head unless specified otherwise.

1) Soft Tissue Stiffness Profile: The force-displacement relationship of human soft tissue is studied through controlled indentation to characterize the non-linear stiffness properties. The indentation carriage moves forward at a constant speed of 9.5 mm/s while force data are recorded in real time. Once the force value crosses a threshold of 8 N, the displacement is recorded and the indenter retracts away from the human limb to its initial position. The indenter pauses for 1s before repeating the process with the same indentation displacement as the first trial. Three trials are performed at each indentation location, spanning 12 angular locations (Fig. 3b) and three rows spaced 25 mm apart along the length of the forearm.

To study the effects of indenter geometry and indentation speed, the stiffness characterization experiment is repeated at six angular locations around the forearm, once with a larger 12 mm diameter cylindrical indenter head, and once with a slower indentation speed of 1.6 mm/s. In addition, the effects of muscle contraction on soft tissue stiffness are explored by instructing the subject to flex their fingers to form a fist while repeating the same indentation experiment at six angular locations around the forearm.

2) Viscoelastic Relaxation: In this experiment, we investigate the viscoelastic properties of human soft tissue. A real-time feedback loop is used to control indenter movement. The indentation carriage moves forward at a constant speed of 6.5 mm/s while force data are recorded in real time. Once the indentation force crosses a threshold of 5 N, the indenter is kept stationary for 10s before it retracts, allowing for viscoelastic relaxation during the 10s window. Three repetitions are performed with a 3s pause in between trials. The viscoelastic relaxation characterization is performed at 6 angular locations around the forearm.

3) Frequency Response Analysis: In this experiment, we investigate the mechanical impedance properties of human soft tissue as described by the measured frequency response. The input is the indentation displacement given as a sine wave with prescribed amplitude and frequency. Indentation force measurements from the single-axis load cell are recorded for 20 cycles. This experiment is conducted at two angular locations, 180° and 330°, which correspond to soft and bony areas, respectively. The indentation displacement amplitude is 0.3125 mm and the frequency is 1.5 Hz. At each location, the indenter tip is brought into contact with the human surface until it registers a force threshold of 2 N.

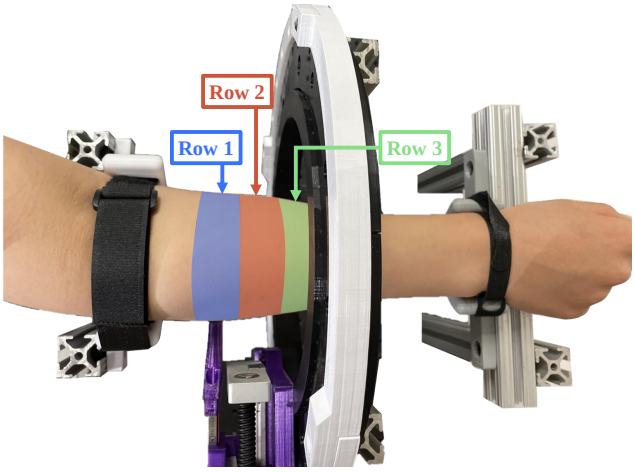

(a) Experimental Setup at 0° Angular Location on Row 1

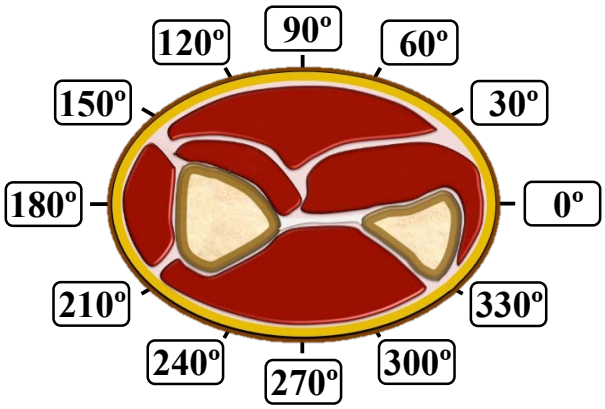

(b) Forearm Cross Section

Fig. 3: The experimental setup shows the indentation location fixed at a point along the length of the arm as well as anchoring cuffs at the wrist and elbow. The 12 angular locations measured in this paper (repeated across the 3 rows highlighted) are shown in the forearm cross section of the right arm, as viewed from the elbow looking out towards the wrist.

IV. Results and Discussion

A. Validation Results

The time series data for force and displacement from the linear indentation carriage are compared to both ground truth measurements, the six-axis load cell and linear position encoder, respectively. Unlike all the other measurements which

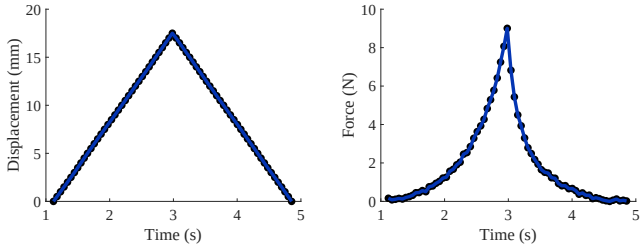

Fig. 4: Raw data collected from instrumentation on the indenter provides indenter head displacement over time (left) and indentation force over time (right). Data shown for 30 degree angular location on the first row.

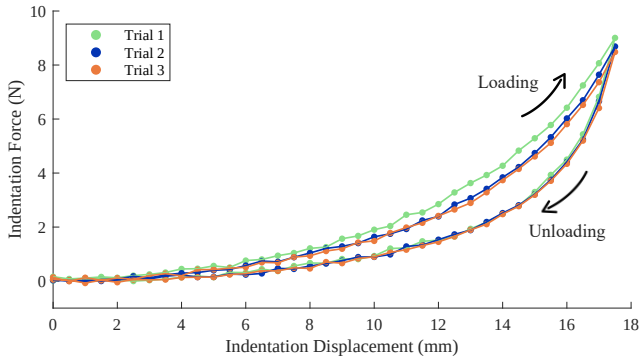

Fig. 5: Force-displacement response from three trials of indentation at the 30 degree angular location on the first row.

are recorded in MATLAB, data from the six-axis load cell are measured through the manufacturer's software and post-processed for time-matching. After comparison, the RMSE for force measurements is 0.109 N and the RMSE for displacement is 0.0112 mm. However, it should be noted that the validation for displacement is limited by the resolution of the linear encoder (0.05 mm).

B. Application Experiments

An example of raw data from the indenter is shown in Fig. 4. The plot for displacement over time shows the constant velocity used during indentation and the plot for force over time shows load cell measurements. When combined, this results in a stiffness profile plotted as indentation force versus indentation displacement. Fig. 5 shows a representative stiffness profile from three repetitions of indentation at one location on the human forearm. A non-linear relationship is observed with hysteresis between loading and unloading. Much of the information in this paper is presented in this format, where a steeper curve corresponds to higher stiffness and a flatter curve corresponds to lower stiffness.

Stiffness profiles at 6 angles out of the 12 locations tested around the forearm are shown in Fig. 6 for the first row (closest to the elbow). Difference in soft tissue stiffness profiles can be observed, especially at 330° where proximity to the ulna bone leads to high stiffness. On the other hand, the lowest stiffness is observed around 180°–240°, areas near muscle bellies which have softer properties. Additionally, each of the 12 angular locations is measured at three rows along the length of the forearm. Different stiffness profiles across rows for three angular locations are shown in Fig. 7. Changes in stiffness across rows are evident at some angular locations such as 0° (Fig. 7), especially in the third row closest to the wrist. Other angular locations, such as 240° (Fig. 7), exhibit minimal difference between rows, indicating that soft tissue properties change differently across the forearm due to underlying muscles and tendons. In these results, the indenter device is able to characterize forearm soft tissue at 36 distinct locations (12 angles across 3 rows), providing a detailed map of stiffness properties.

At 6 angular locations on the first row, we also investigated the difference in stiffness profiles between a relaxed forearm and a flexed forearm (Fig. 8). As expected, significantly higher stiffness is observed during the flexed case at every angular location resulting from the contraction of underlying muscles in the forearm. This effect is least apparent at angular locations where the soft tissue is already stiff (0° in Fig. 8) and most apparent at locations where muscle contraction occurs (180° in Fig. 8). Thus, any application that considers soft tissue properties must account for how stiffness increases from muscle activation. We also investigated the effects of indentation speed and indenter head geometry, both of which did not show significant differences or trends. While more testing is necessary to confirm these observations, the results align with previous findings [14], [17] and highlight which variables are less important to control in the design of soft tissue characterization experiments.

The results from the viscoelastic relaxation experiment are shown in Fig. 9 for 2 of the 6 angles measured in the first row. The viscoelastic behavior can be observed during the 10s window when indentation displacement is held constant and dynamic effects dissipate as the indentation force approaches steady-state, specifically in the first 2-3s. This characterization can be used to develop viscoelastic models of the soft tissue response, as done in past literature with the use of a shear relaxation function [14]. Information about dynamic soft tissue properties can help predict how interaction behavior in a wearable interface will change over time after it is initially donned on a human user.

The frequency response of human soft tissue at the 180° location is shown in Fig. 10 for the first 10 cycles out of the 20 total oscillations. The same test was also conducted at the 330° angular location. Different soft tissue properties not only affect the amplitude gain but also determine the lower frequency oscillations and phase margin. Averaged across 20 cycles, the output amplitude was 0.0844 N at 180° and 0.353 N at 330°. Existing research has shown that such response behavior changes depend on the input frequency and initial indentation pressure [5]. This type of characterization is useful for understanding haptic perception and detection thresholds at the human skin [5], [7].

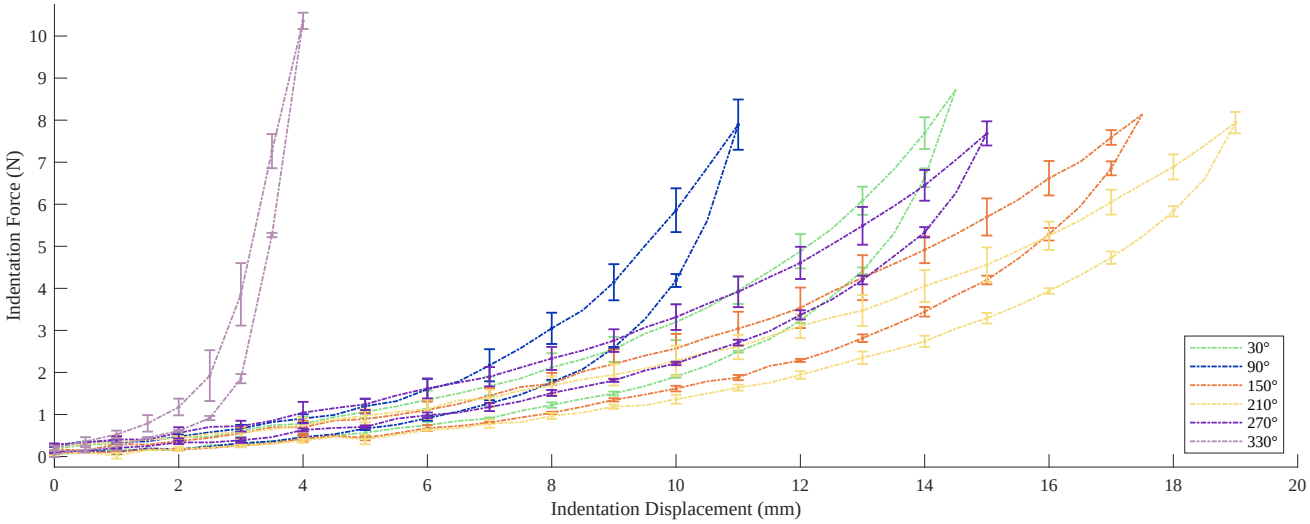

Fig. 6: Force-displacement response at 6 angular locations on the first row of the forearm for a single human subject.

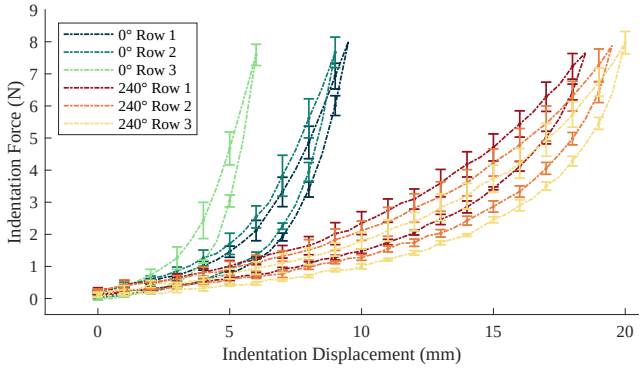

Fig. 7: Force-displacement response for three rows at two angular locations. Row 1 is closest to the elbow and row 3 is closest to the wrist.

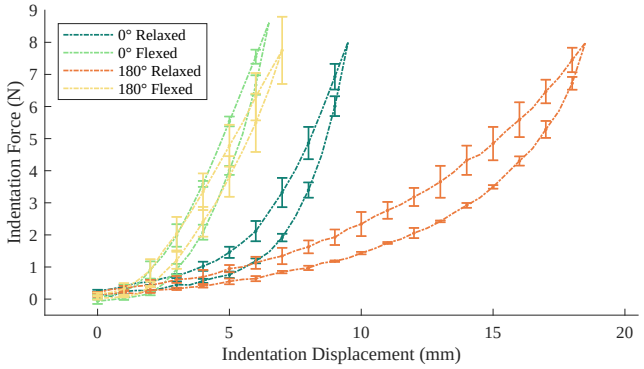

Fig. 8: Force-displacement response with the forearm relaxed and flexed at two angular locations. Higher stiffness is observed at all angular locations during the flexed case when muscles are co-contracted.

C. Human-Centered Design and Analysis

Given the different types of soft tissue characterizations possible, the indenter presented here is an ideal tool for motivating a human-centered approach to the design and analysis

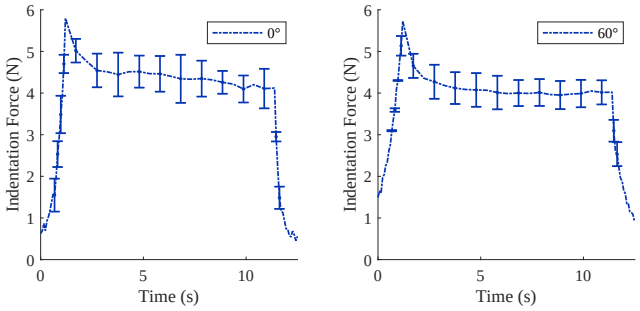

Fig. 9: Viscoelastic relaxation response at two angles.

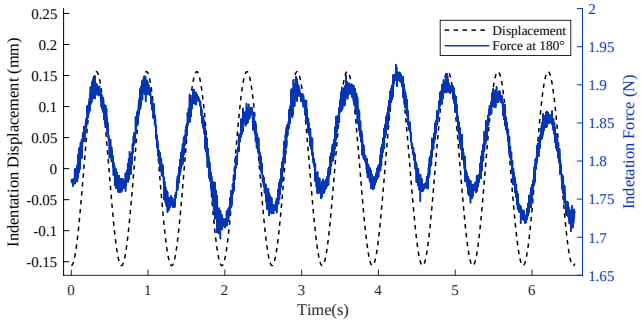

Fig. 10: Indentation force in response to a sinusoidal input displacement at the 180° angular location.

of attachment interfaces in wearable robotic devices. Although tissue properties vary across a human limb, most wearable attachments use the same padding material at the interface surface, which can cause discomfort at bony prominences that have higher soft tissue stiffness. To incorporate human characterization in the design process, the measurement of stiffness profiles can be used to create variable stiffness pHRI attachments such that softer areas on the human interface with stiffer areas on the attachment and vice versa, known as impedance matching [2]. As an example, the stiffness values shown in Fig. 11a for 12 angles on the first row are estimated as the slope of a linear regression for the second

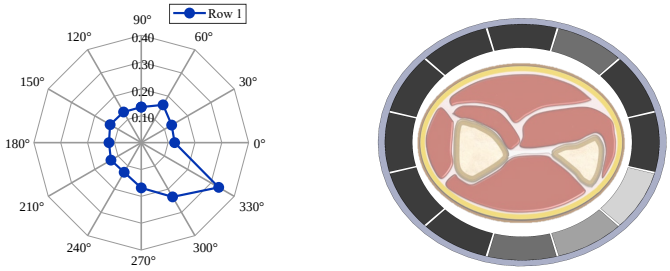

(a) Arm Stiffness (b) Proposed Interface Design

Fig. 11: Human-centered approach for interface design in which interface padding properties are varied depending on stiffness measurements of the human limb.

half of the unloading force-displacement data. The proposed interface design (Fig. 11b) uses an inverse stiffness matching approach [2] in which padding of different stiffness is used around the interface surface. Each shaded panel in Fig. 11b represents a discretized padding element where lighter shading corresponds to softer padding and darker shading corresponds to stiffer padding.

In addition to design, characterization from the indenter is also valuable for modeling and analysis of the interaction at human-robot interfaces. The stiffness and viscoelastic relaxation properties of human soft tissue can be used to build simulations that predict interaction behavior for different loading conditions [1], elucidating how relative motion and interface pressure distributions can change based on design and control choices. The experiments showing differences in soft tissue stiffness for relaxed and flexed muscles highlights the need for considering the dynamic changes in biomechanical properties during motion and task performance. The indenter's frequency response experiment can be used to study detection thresholds for human perception, going a step deeper to show how interaction with a wearable robotic device will be recognized by a user's nervous system.

V. Conclusions and Future Work

The validation and experiments with the actuated indenter presented in this paper confirm its value as a tool for the measurement of different soft tissue properties which play a critical role in determining pHRI behavior. The actuated control of indentation displacement along with force feedback allows for the implementation of a variety of experimental protocols that allows for the characterization of stiffness, viscoelasticity, and detection thresholds of human soft tissue. With many types of biomechanical measurements possible through one device, the indenter sets the foundation for designing attachment interfaces and modeling pHRI through a new perspective that prioritizes the human user. This human-centered approach will pave the way for wearable robotic devices that seamlessly integrate with their users and optimize their functionality.

Future studies will utilize the indenter device to perform human subject experiments that can reveal general trends in soft tissue properties. This information can be used to build models for predicting viscoelastic behavior of human soft tissue and develop ergonomic interfaces for wearable devices. The applications of the indenter can be extended to other human limbs such as the upper arm and the lower leg. Results from indentation experiments can also be combined with other instrumentation such as electromyography (EMG) and MRI for more in-depth characterization of soft tissue.

References

[1] R. J. Varghese, G. Mukherjee, R. King, S. Keller, and A. D. Deshpande, "Designing variable stiffness profiles to optimize the physical human robot interface of hand exoskeletons," in *2018 7th IEEE International Conference on Biomedical Robotics and Biomechatronics (Biorob)*. IEEE, 2018, pp. 1101–1108.

[2] D. M. Sengeh and H. Herr, "A variable-impedance prosthetic socket for a transtibial amputee designed from magnetic resonance imaging data," *JPO: Journal of Prosthetics and Orthotics*, vol. 25, no. 3, pp. 129–137, 2013.

[3] R. B. Groves, S. A. Coulman, J. C. Birchall, and S. L. Evans, "An anisotropic, hyperelastic model for skin: experimental measurements, finite element modelling and identification of parameters for human and murine skin," *Journal of the mechanical behavior of biomedical materials*, vol. 18, pp. 167–180, 2013.

[4] Y. Liu, A. E. Kerdok, and R. D. Howe, "A nonlinear finite element model of soft tissue indentation," in *International Symposium on Medical Simulation*. Springer, 2004, pp. 67–76.

[5] S. J. Bolanowski Jr, G. A. Gescheider, R. T. Verrillo, and C. M. Checkosky, "Four channels mediate the mechanical aspects of touch," *The Journal of the Acoustical society of America*, vol. 84, no. 5, pp. 1680–1694, 1988.

[6] K. A. Richardson, T. T. Imhoff, P. Grigg, and J. J. Collins, "Using electrical noise to enhance the ability of humans to detect subthreshold mechanical cutaneous stimuli," *Chaos: An Interdisciplinary Journal of Nonlinear Science*, vol. 8, no. 3, pp. 599–603, 1998.

[7] D. Ferrington, B. Nail, and M. Rowe, "Human tactile detection thresholds: modification by inputs from specific tactile receptor classes," *The Journal of physiology*, vol. 272, no. 2, pp. 415–433, 1977.

[8] Y.-P. Zheng and A. F. Mak, "An ultrasound indentation system for biomechanical properties assessment of soft tissues in-vivo," *IEEE transactions on biomedical engineering*, vol. 43, no. 9, pp. 912–918, 1996.

[9] H. Oflaz and O. Baran, "A new medical device to measure a stiffness of soft materials," *Acta of bioengineering and biomechanics*, vol. 16, no. 1, 2014.

[10] A. Petron, J.-F. Duval, and H. Herr, "Multi-indenter device for in vivo biomechanical tissue measurement," *IEEE Transactions on Neural Systems and Rehabilitation Engineering*, vol. 25, no. 5, pp. 426–435, 2016.

[11] D. Oh, S. Lee, and Y. Choi, "Simultaneous stiffness measurement device for a human forearm," *IEEE Access*, vol. 8, pp. 15 313–15 321, 2020.

[12] S. Xiong, R. S. Goonetilleke, C. P. Witana, and W. Rodrigo, "An indentation apparatus for evaluating discomfort and pain thresholds in conjunction with mechanical properties of foot tissue in vivo." *Journal of Rehabilitation Research & Development*, vol. 47, no. 7, 2010.

[13] D. Oh, S. Lee, and Y. Choi, "Development of 6-axis stiffness measurement device for prosthetic socket design," *The Journal of Korea Robotics Society*, vol. 14, no. 1, pp. 58–64, 2019.

[14] E. Samur, M. Sedef, C. Basdogan, L. Avtan, and O. Duzgun, "A robotic indenter for minimally invasive measurement and characterization of soft tissue response," *Medical Image Analysis*, vol. 11, no. 4, pp. 361–373, 2007.

[15] C. Pailler-Mattei, S. Bec, and H. Zahouani, "In vivo measurements of the elastic mechanical properties of human skin by indentation tests," *Medical engineering & physics*, vol. 30, no. 5, pp. 599–606, 2008.

[16] D. H. Jones, R. D. Kilgour, and A. S. Comtois, "Test-retest reliability of pressure pain threshold measurements of the upper limb and torso in young healthy women," *The Journal of Pain*, vol. 8, no. 8, pp. 650–656, 2007.

[17] B. Ahn and J. Kim, "Measurement and characterization of soft tissue behavior with surface deformation and force response under large deformations," *Medical image analysis*, vol. 14, no. 2, pp. 138–148, 2010.